

The Structure of Aqueous Guanidinium Chloride Solutions

Philip E. Mason,[†] George W. Neilson,[‡] John E. Enderby,[‡] Marie-Louise Saboungi,^{||}
Christopher E. Dempsey,[§] Alexander D. MacKerell, Jr.,[⊥] and John W. Brady*[†]

Contribution from the Department of Food Science, Stocking Hall, Cornell University, Ithaca, New York 14853, H. H. Wills Physics Laboratory, University of Bristol, BS8 1TL, U.K., Department of Biochemistry, University of Bristol, BS8 1TD, U.K., Centre de Recherche sur la Matière Divisée, 1 bis rue de la Férollerie, 45071 Orléans, France, and School of Pharmacy, University of Maryland, 20 Penn Street, Baltimore, Maryland 21201

Received January 30, 2004; E-mail: jwb7@cornell.edu

Abstract: The combination of neutron diffraction with isotopic substitution (NDIS) experiments and molecular dynamics (MD) simulations to characterize the structuring in an aqueous solution of the denaturant guanidinium chloride is described. The simulations and experiments were carried out at a concentration of 3 *m* at room temperature, allowing for an examination of any propensity for ion association in a realistic solution environment. The simulations satisfactorily reproduced the principal features of the neutron scattering and indicate a bimodal hydration of the guanidinium ions, with the N–H groups making well-ordered hydrogen bonds in the molecular plane, but with the planar faces relatively deficient in interactions with water. The most striking feature of these solutions is the rich ion–ion ordering observed around the guanidinium ion in the simulations. The marked tendency of the guanidinium ions to stack parallel to their water-deficient surfaces indicates that the efficiency of this ion as a denaturant is due to its ability to simultaneously interact favorably with both water and hydrophobic side chains of proteins.

Introduction

It has been more than a century since Hofmeister first ordered cations and anions into series according to their effects on protein solubility and stability, and, although some progress has been made in recent years,^{1–3} the atomic-scale mechanisms for these effects are still incompletely understood. For simple monatomic cations, this ordering can be rationalized in terms of the effect that water binding to ions of various radii and surface charge densities has on the solution surface tension. For the more interesting case of structurally complex molecular ions such as thiocyanate and guanidinium, the mechanism is less clear. It has long been assumed that Hofmeister rankings arise from differing effects of the various ions on the structure of liquid water, with some solutes labeled as “structure makers” and others labeled “structure breakers”.^{4,5} Recent studies have indicated that neutral molecular solutes do indeed impose considerable structure on their first hydration shell water molecules. Molecular solutes typically have several functional groups with differing solvation requirements juxtaposed in close proximity by the molecular structure, and the overlapping

hydration interactions of these neighboring groups result in complex solvent structuring patterns that are characteristic of the specific solute molecular architecture.^{6–8}

Just how far out into the solvent, away from the solute, these perturbed structural patterns extend remains unclear. It has been hypothesized that some solutes interact with the underlying structure of liquid water better than others, as in various sugar structural isomers,^{9,10} but such theories seem to require an assumption that liquid water has a long-range ordering which in some way resembles hexagonal ice I_h.^{11,12} A recent femto-second mid-infrared spectroscopic measurement of orientational correlation times in aqueous ionic solutions suggest that there is no effect of the ions on the bulk water structure beyond the first hydration shell; that is, there is neither an increase nor a decrease in water structuring due to the presence of the ions.¹³ A similar result was found in a recent neutron diffraction study of the neutral but polar D-glucose in solution,¹⁴ even though sugars are usually considered to be weak structure-makers.⁴

[†] Cornell University.

[‡] H. H. Wills Physics Laboratory, University of Bristol.

[§] Department of Biochemistry, University of Bristol.

^{||} Centre de Recherche sur la Matière Divisée.

[⊥] University of Maryland.

(1) Parsegian, V. A. *Nature* **1995**, *378*, 335–336.

(2) Baldwin, R. L. *Biophys. J.* **1996**, *71*, 2056–2063.

(3) Mason, P. E.; Neilson, G. W.; Dempsey, C. E.; Barnes, A. C.; Cruickshank, J. M. *Proc. Natl. Acad. Sci. U.S.A.* **2003**, *100*, 4557–4561.

(4) Franks, F. In *Water: A Comprehensive Treatise*; Franks, F., Ed.; Plenum Press: New York, 1973; Vol. 2, pp 1–54.

(5) Ohtaki, H.; Radnai, T. *Chem. Rev.* **1993**, *93*, 1157–1204.

(6) Sidhu, K. S.; Goodfellow, J. M.; Turner, J. Z. *J. Chem. Phys.* **1999**, *110*, 7943–7950.

(7) Liu, Q.; Brady, J. W. *J. Am. Chem. Soc.* **1996**, *118*, 12276–12286.

(8) Schmidt, R. K.; Karplus, M.; Brady, J. W. *J. Am. Chem. Soc.* **1996**, *118*, 541–546.

(9) Galema, S. A.; Hoiland, H. *J. Phys. Chem.* **1991**, *95*, 5321–5326.

(10) Galema, S. A.; Howard, E.; Engberts, J. B. F. N.; Grigera, J. R. *Carbohydr. Res.* **1994**, *265*, 215–225.

(11) Suggitt, A. In *Water: A Comprehensive Treatise*; Franks, F., Ed.; Plenum: New York, 1975; Vol. 4, pp 519–567.

(12) Mashimo, S.; Miura, N.; Umehara, T. *J. Chem. Phys.* **1992**, *97*, 6759–6765.

(13) Omta, A. W.; Kropman, M. F.; Woutersen, S.; Bakker, H. J. *Science* **2003**, *301*, 347–349.

(14) Mason, P. E.; Neilson, G. W.; Barnes, A. C.; Enderby, J. E.; Brady, J. W.; Saboungi, M.-L. *J. Chem. Phys.* **2003**, *119*, 3347–3353.

It does seem possible, however, that for some solutes the direct ("first hydration shell") solvent structuring patterns required to optimally hydrate the various functional groups might require no significant long-range structuring beyond that found in pure water. Moreover, it has been recognized that some polar and even ionic solutes may affect protein stability and solubility by directly or indirectly binding to protein functional groups or liberating water molecules from contact with hydrophobic surfaces.^{15,16} It has become clear that understanding the effects of molecular solutes on protein behavior in solution will require a detailed picture of the interaction of water molecules with the specific molecular architecture of the solutes.

Neutron scattering experiments have been extremely powerful in revealing the water structuring around simple monatomic ions,^{17–19} noble gases,^{20,21} and molecular species with quasi-spherical symmetry such as tetramethylammonium.^{22,23} The measured scattering is a direct function of the structure of the solution, even if it is difficult or sometimes not possible to interpret for complex molecules. Molecular Mechanics (MM) simulations, on the other hand, provide complete detail about a model system, allowing qualitative interpretation of the nature of the structuring, but this model mimics the real system only as closely as the force fields and other approximations mimic the actual structures and energetics of the system. However, in combination, the neutron scattering data can provide a demanding test for the quantitative accuracy of the approximations in the simulations, and the rich structural detail of the simulations allows for atomistic interpretation of the scattering data.²⁴ We report here such a paired neutron diffraction experiment and molecular dynamics simulation study of aqueous solutions of the important biological species guanidinium with chloride counterions at typical denaturing concentrations.

The guanidinium ion (Gdm^+) is an ideal model for the investigation of the hydration of complex molecular species in solution due to its highly symmetrical and rigid structure. The biological importance of the Gdm^+ ion stems from at least two sources. First, it is a functional analogue for part of the side chain of the amino acid arginine, and the interaction of this moiety with water and other species can give insight into the factors underlying protein folding. This ion is also an important tool in the thermodynamic study of protein folding and denaturation, where it is commonly used as a powerful denaturant (usually as the chloride or thiocyanate salt).²⁵ Furthermore, because Gdm^+ has both a hydrogen-bonding NH_2 functionality and a non-hydrogen-bonding carbon atom, the ion makes an archetypal system for the study of how biological molecules hydrate.

Guanidinium ions have been studied previously using Molecular Mechanics simulations. Boudon et al. used Monte Carlo

(MC) simulations to calculate a potential of mean force (PMF) for two guanidinium ions in a TIP4P water solution with a guanidinium force field based on ab initio calculations.²⁶ Subsequently, further MC studies using the TIP3P and SPC water models and a polarizable model found a quantitative dependence of the calculated results on the water model,²⁷ but all four simulations in fact found a tendency for the ions to associate in aqueous solution, with only the strength of this association varying between the models. The chloride counterions have also been separately studied previously and were once thought to also pair,^{28,29} but this was only observed experimentally in highly concentrated ($>8\text{ m}$) solutions of lithium chloride³⁰ and was not observed in aqueous solutions of 4.3 m nickel chloride.¹⁸

Methods

Experimental Procedures. Experimental samples were prepared in the following manner. Isotopic HCl was produced by the action of 98% H_2SO_4 on NaCl under high vacuum. After double distillation, the HCl was dissolved in D_2O and calibrated versus a standard NaOH solution. In all cases, both isotopic acids were calibrated versus the same NaOH standard. Starting with pure NaCl and on scales $>1\text{ g}$, the method reproducibly produced yields $>95\%$. To identical portions of the $\text{Gdm}_2\text{-CO}_3$ (from a single volumetric D_2O solution) was added ca. a 10% excess of the relevant isotopic acid to produce the relevant salts. The excess acid was recovered by distillation, and titrated versus volumetric NaOH. Samples were then exchanged of any remaining protium by several washings with D_2O under high vacuum. Finally, the appropriate amount of D_2O was added gravimetrically (while maintaining high vacuum) to effect the correct concentration, and the sample was sealed under high vacuum in an all-glass ampule. D_2O was used because deuterium does not have the high incoherent scattering of protium. Also, the M–H correlation (where M is the substituted nuclei), which usually constitutes about 60% of the total contrast, is about twice as large in D_2O as compared to H_2O due to deuterium having about twice the magnitude of scattering length as protium. $^{15}\text{N}_3\text{-GdmCl}$ was purchased from Aldrich. All exchangeable hydrogen atoms were removed by the procedure described above.

The difference methods of NDIS are well established in the literature;³¹ we only reproduce those parts that are relevant to the work undertaken here. The main tenet of the method is that there is complete isomorphism between isotopically labeled samples of the same chemical compound. Solutions of guanidinium chloride were prepared by dissolving the solute in heavy water in exactly the ratio of 3 mol of each of the various isotopically labeled solutes to 55.5 mol of D_2O , hereafter referred to as 3 m solutions for convenience. Total neutron scattering patterns (corrected for multiple scattering and absorption) were obtained for these solutions of Gdm^{35}Cl , Gdm^{37}Cl , $^{15}\text{N}_3\text{-GdmCl}$, and GdmCl (in D_2O at 300 K) on the SANDALS diffractometer at the ISIS spallation source of the Rutherford Appleton Laboratory (RAL). In each case, the samples were loaded into flat plate sample containers with 1 mm thick walls of null-scattering Ti/Zr and a sample thickness of 1 mm. Application of the first-order difference method of NDIS to these four patterns gave the total pair distribution functions $^aG_N(r)$ and $^bG_{\text{Cl}}(r)$ for the nitrogen atoms on Gdm^+ and Cl^- , respectively. These may be written explicitly as:

- (15) Kuharski, R. A.; Rossky, P. J. *J. Am. Chem. Soc.* **1984**, *106*, 5794–5800.
- (16) Kuharski, R. A.; Rossky, P. J. *J. Am. Chem. Soc.* **1984**, *106*, 5786–5793.
- (17) Enderby, J. E.; Neilson, G. W. *Rep. Prog. Phys.* **1981**, *44*, 593–653.
- (18) Neilson, G. W.; Enderby, J. E. *Proc. R. Soc. London* **1983**, *A390*, 353–371.
- (19) Neilson, G. W.; Enderby, J. E. *Adv. Inorg. Chem.* **1989**, *34*, 195–218.
- (20) Broadbent, R. D.; Neilson, G. W. *J. Chem. Phys.* **1994**, *100*, 7543–7547.
- (21) Sullivan, D. M.; Neilson, G. W.; Fischer, H. E. *J. Chem. Phys.* **2001**, *115*, 339–343.
- (22) Barnes, A. C.; Neilson, G. W.; Enderby, J. E. *J. Mol. Liq.* **1995**, *65/66*, 99–106.
- (23) Turner, J. Z.; Soper, A. K.; Finney, J. L. *J. Chem. Phys.* **1995**, *102*, 5438–5443.
- (24) Soper, A. K.; Luzar, A. *J. Phys. Chem.* **1996**, *100*, 1357–1367.
- (25) Azuaga, A. I.; Canet, D.; Smeenk, G.; Berends, R.; Titgemeijer, F.; Duurkens, R.; Mateo, P. L.; Scheek, R. M.; Robillard, G. T.; Dobson, C. M.; van Nuland, N. A. *J. Biochemistry* **2003**, *42*, 4883–4895.

- (26) Boudon, S.; Wipff, G.; Maigret, B. *J. Phys. Chem.* **1990**, *94*, 6056–6061.
- (27) Soetens, J.-C.; Millot, C.; Chipot, C.; Jansen, G.; Angyán, J. G.; Maigret, B. *J. Phys. Chem. B* **1997**, *101*, 10910–10917.
- (28) Pettitt, B. M.; Rossky, P. J. *J. Chem. Phys.* **1986**, *84*, 5836–5844.
- (29) Dang, L. X.; Pettitt, B. M. *J. Chem. Phys.* **1987**, *86*, 6560–6561.
- (30) Ansell, S.; Neilson, G. W. *J. Chem. Phys.* **2000**, *112*, 3942–3944.
- (31) Neilson, G. W.; Enderby, J. E. *J. Phys. Chem.* **1996**, *100*, 1317–1322.

$${}^nG_N(r) = [12.36g_{\text{NH}}(r) + 4.56g_{\text{NO}}(r) + 1.12g_{\text{NN}}(r) + 0.31g_{\text{NC}}(r) + 0.45g_{\text{NCI}}(r)]/18.80 \quad (1)$$

$${}^nG_{\text{Cl}}(r) = [11.13g_{\text{ClH}}(r) + 4.16g_{\text{ClO}}(r) + 1.09g_{\text{ClN}}(r) + 0.26g_{\text{ClC}}(r) + 0.29g_{\text{ClCl}}(r)]/16.92 \quad (2)$$

where n represents that these functions have been normalized by division by the sum of the scattering prefactors, and $g_{ab}(r)$ is the radial pair distribution function of atoms a and b .

Computational Procedures. In the MD simulations, a neutral periodic cubic system was created at 3 m concentration containing a number of independent guanidinium cations and chloride counterions surrounded by explicit water molecules. The simulations employed a solute potential energy function based on the parameters for arginine in the CHARMM22 protein force field,³² with the atomic partial charges assigned symmetrically (atom charges: C 0.64; N -0.80; H 0.46). Water molecules were represented using the TIP3P model.³³ All simulations were performed using the CHARMM program,³⁴ with chemical bonds to hydrogen atoms kept fixed using SHAKE³⁵ and a time step of 1 fs. Arbitrary starting coordinates were generated by randomly placing and orienting 48 Gdm molecules and 48 chloride ions in a cubic box with sides of 34 Å. These coordinates were superimposed on a box of 1296 water molecules, and those which were within 2.77 Å of any solute heavy atom were discarded, with this distance chosen so as to produce a system with the correct concentration. By design, this procedure produced a 3 m solution (48 GdmCl in 882 TIP3P water molecules, 3.02 m). Finally, the box length was rescaled to 31.7894 Å; this yielded the correct physical number density (0.0988 atoms Å⁻³).

The van der Waals interactions were smoothly truncated on an atom-by-atom basis using switching functions from 10.5 to 11.5 Å,³⁴ while electrostatic interactions were treated using the Ewald method³⁶ with a real space cutoff of 12.5 Å, $\kappa = 0.333$, and a K_{max}^2 of 27. Initial velocities were assigned from a Boltzmann distribution (300 K) followed by 5 ps of equilibration dynamics with velocities being reassigned every 0.1 ps. The simulation was then run for 800 ps with no further velocity reassignment. The first 300 ps of this was taken as equilibration, and the remaining 500 ps was used for analysis. Subsequently, ${}^nG_N(r)$ and ${}^nG_{\text{Cl}}(r)$ were obtained by summing the calculated pair correlation functions (weighted by the scattering prefactors shown in eqs 1 and 2).

To test the sensitivity of the simulation results to the various approximations, a series of additional simulations were conducted. After comparing the results of the first preliminary simulation to the scattering data, a revised guanidinium intramolecular force field was developed (see below) and tested in a second 800 ps simulation. For reasons discussed below, this simulation became the primary data set used for analysis as the best computational model. A shorter simulation was also conducted with completely rigid guanidinium ions. In addition, the sensitivity to water model was tested by conducting another 800 ps simulation using the SPC/E water model with the original solute force field. Finally, the stability of the Ewald summation was tested by repeating the simulation using a κ of 0.36 and a K_{max}^2 of 27.

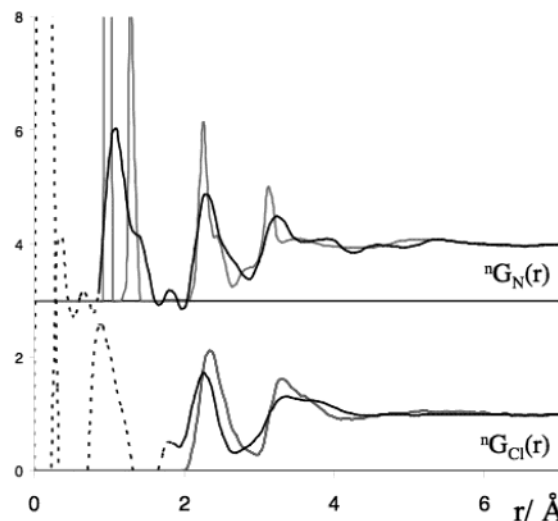


Figure 1. The comparison of NDIS measurements to MD. (a) ${}^nG_N(r)$ as measured by NDIS (black line), and calculated from MD simulation (using the revised force constants, gray line). (b) ${}^nG_{\text{Cl}}(r)$ as measured by NDIS (black line), and calculated by MD simulation (gray line). The dotted black line represents where the NDIS data become unphysical.

Results

The functions ${}^nG_N(r)$ and ${}^nG_{\text{Cl}}(r)$ as determined by NDIS and as calculated from the MD simulation are shown in Figure 1. For ${}^nG_N(r)$, the main difference between these two functions is that the MD produces very sharp peaks for the NH and NC bonds (at 1.0 and 1.4 Å, respectively), while the NDIS measurement has considerably broader, resolution-limited features at these positions. The peak at 2.3 Å is due to the intramolecular NN and NH correlations, while the peak at 3.1 Å is due, in part, to an intramolecular NH correlation. ${}^nG_{\text{Cl}}(r)$ has been measured for several concentrations and counterions, and it has been found to be remarkably insensitive to both concentration (at less than ca. 6 m) and counterion³⁷ (other than those that form molecular species such as Zn³⁸). It is therefore not surprising that the ${}^nG_{\text{Cl}}(r)$ measured here is very similar to previously determined structure factors obtained by NDIS for the chloride ion in aqueous solution. The general form of the chloride hydration consists of a Cl–H correlation at 2.3 Å, with correlations of the chloride to the remaining OH of the water occurring at about 3.3 Å.³⁹

If the MD result is back Fourier transformed to $S(Q)$, and retransformed using the cutoffs of the experimental data (imposing the experimental resolution on the MD data), it is found that the peaks at about 2.1 and 2.6 Å are still somewhat too sharp. This suggests that the guanidinium force field parameters used here (which were taken from the standard CHARMM parameters for arginine) might be somewhat too rigid. To explore this possibility, an alternate set of bond stretching and bending parameters was developed (see Tables 1 and 2 of the Supporting Information) based on ab initio calculations at the scaled MP2/6-311G** level. In fact, the new parameters are slightly more rigid than the original set. New simulations were subsequently conducted using these new

(32) MacKerell, A. D.; Bashford, D.; Bellott, M.; Dunbrack, R. L.; Evanseck, J. D.; Field, M. J.; Fischer, S.; Gao, J.; Guo, H.; Ha, S.; Joseph-McCarthy, D.; Kuchnir, L.; Kuczera, K.; Lau, F. T. K.; Mattos, C.; Michnick, S.; Ngo, T.; Nguyen, D. T.; Prodhom, B.; Reiher, W. E.; Roux, B.; Schlenkrich, M.; Smith, J. C.; Stote, R.; Straub, J.; Watanabe, M.; Wiorkiewicz-Kuczera, J.; Yin, D.; Karplus, M. *J. Phys. Chem. B* **1998**, *102*, 3586–3616.

(33) Jorgensen, W. L.; Chandrasekhar, J.; Madura, J. D.; Impey, R. W.; Klein, M. L. *J. Chem. Phys.* **1983**, *79*, 926–935.

(34) Brooks, B. R.; Brucoleri, R. E.; Olafson, B. D.; Swaminathan, S.; Karplus, M. *J. Comput. Chem.* **1983**, *4*, 187–217.

(35) van Gunsteren, W. F.; Berendsen, H. J. C. *Mol. Phys.* **1977**, *34*, 1311–1327.

(36) Darden, T.; York, D.; Pedersen, L. J. *J. Chem. Phys.* **1993**, *98*, 10089–10092.

(37) Neilson, G. W.; Mason, P. E.; Ramos, S.; Sullivan, D. *Philos. Trans. R. Soc. London* **2001**, *A359* (1785), 1575–1591.

(38) Powell, D. H.; Gullidge, P. M. N.; Neilson, G. W.; Bellissent-Funel, M.-C. *Mol. Phys.* **1990**, *71*, 1107–1116.

(39) Powell, D. H.; Neilson, G. W.; Enderby, J. E. *J. Phys.: Condens. Matter* **1993**, *5*, 5723–5730.

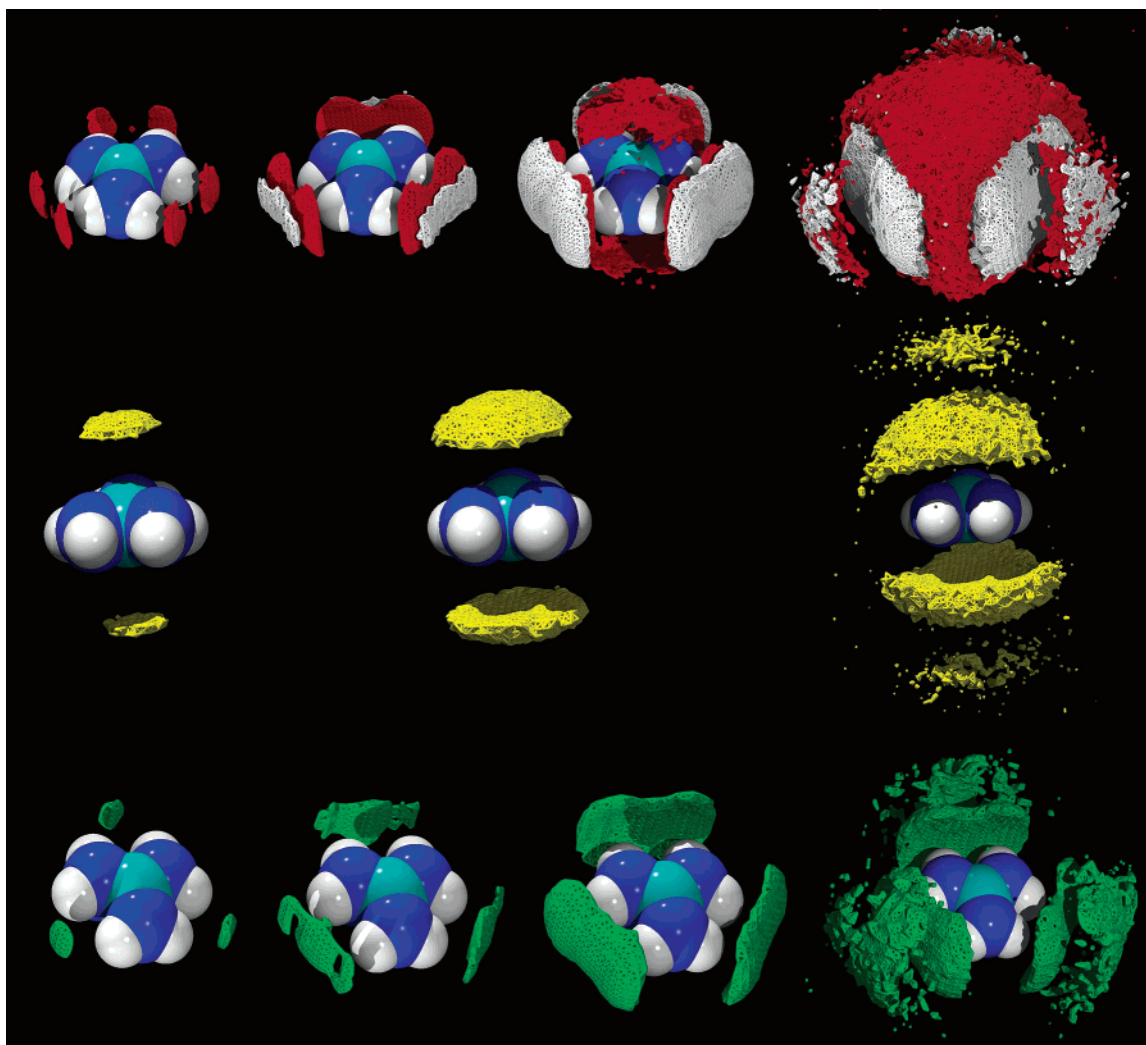


Figure 2. Top: density maps of H(water) and O around the Gdm^+ ion. Middle: density maps of C around the Gdm^+ ion. Lower: density maps of Cl^- around the Gdm^+ ion. Top (O, red), from left to right, 0.250, 0.100, 0.055, and 0.038 atoms \AA^{-3} (9.2, 3.7, 2.0, and 1.4 times the average number density of the O atom); and (H(water), white) from left to right, 0.500, 0.200, 0.110, and 0.076 atoms \AA^{-3} (9.2, 3.7, 2.0, and 1.4 times the average number density of the H(water) atom). Middle: (C, yellow), from left to right, 0.012, 0.006, and 0.003 atoms \AA^{-3} (8.1, 4, and 2 times the average number density of the carbon atom). Lower: (Cl, green), from left to right, 0.1, 0.04, 0.01, and 0.0035 atoms \AA^{-3} (68, 27, 6.8, and 2.4 times the average number density of the chloride ion).

parameters, and it was found that the intermolecular structure is relatively insensitive to valence parameters. The resolution of the diffraction data is not sufficient to distinguish between the two simulations, and the broadening of the experimental peaks is the result of resolution and instrument limitations. However, because the new parameters give a better fit to the vibrational spectrum for guanidinium, the primary simulations used in the analyses reported here were the ones employing these new parameters. Given that both ${}^nG_{\text{N}}(r)$ and ${}^nG_{\text{Cl}}(r)$ calculated from this trajectory are in reasonable agreement with the experimental measurement, it follows that this trajectory gives an accurate representation of the physical system, at least by these criteria.

Thus validated, this trajectory was subjected to further analysis to determine the density of atomic species around the Gdm^+ ion, as measures of the structure imposed on the solutions. Traditionally, the average structure of aqueous solutions is analyzed in terms of spherically averaged radial distribution functions because such functions can be directly compared to experimental data. However, for molecular solutes, and in

particular for complex polyfunctional biological molecules, the radial averaging in such pair distributions obscures important details of the actual average arrangement of water molecules around the molecular structure.⁷ The advantage of MM simulations is that the full anisotropic correlation can be computed and analyzed in terms of the structure imposed jointly by more than one atom or functional group.^{7,8,40} Both types of distribution have been calculated from the present MD simulations to characterize the interaction of the three components in the solution.

The top panel in Figure 2 displays the three-dimensional simulated anisotropic distribution of water oxygen and hydrogen densities around the Gdm^+ solute, represented using the VMD molecular graphics program.⁴¹ There is a strong tendency for the water molecules to make linear hydrogen bonds as acceptors for the guanidinium hydrogen atoms, as can be seen from Figure 3, which displays the distribution of hydrogen bond angles for

(40) Brady, J. W. *Forefronts/Cornell Theory Center* **1993**, 9, 7.

(41) Humphrey, W.; Dalke, A.; Schulten, K. *J. Mol. Graphics* **1996**, 14, 33–38.

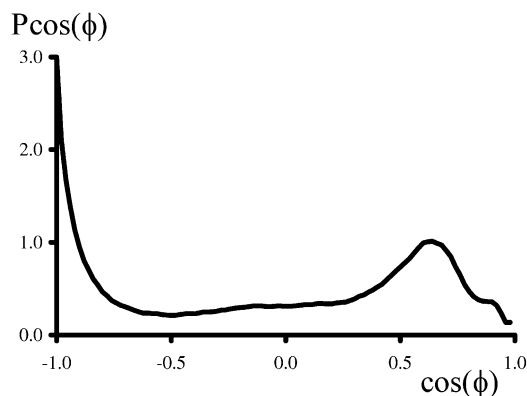


Figure 3. Distribution of hydrogen bond angles for water molecules bound to guanidinium ions as calculated from the MD simulations for all water molecules where the N–O distance was less than 3.5 Å.

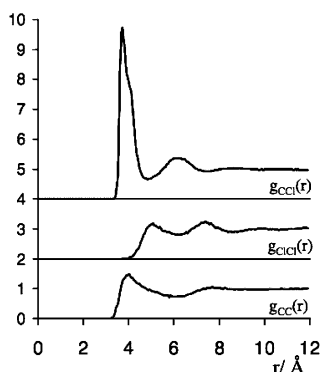


Figure 4. The radial distribution functions $g_{CCl}(r)$ (top), $g_{ClCl}(r)$ (middle), and $g_{OO}(r)$ (lower).

the water–guanidinium hydrogen bonds. The secondary peak in this distribution around $\cos(\phi) \approx 0.65$, corresponding to a ϕ of approximately 50° , results from the second proton of each NH_2 group, because if one is making a linear hydrogen bond to a water oxygen atom, then the other proton will be approximately at this angle. Because of the linearity of these hydrogen bonds, the water molecules are strongly constrained to remain in the plane of the Gdm^+ ion. By direct averaging, there are approximately 4.5 such hydrogen-bonded water molecules per Gdm^+ , while in principle there could be six such partners (albeit slightly distorted due to steric constraints). However, from the bottom panel of Figure 2, which displays the density of chloride ions, it is clear that there is competition for these sites by the chloride ions. This chloride ordering is a response to the 6 hydrogen atoms with partial positive charges around the equatorial periphery of the molecule. The total average hydration number of the guanidinium ion is approximately 9.9, counting all water molecules within either 3.5 Å of a nitrogen atom or 4.6 Å of a carbon atom, with approximately three weakly bound water molecules structuring above or below the carbon atom in a diffuse cloud. Despite the relatively high charge of the carbon atoms, their large radius prevents them from hydrogen bonding, and these faces behave like hydrophobic surfaces in the way water structures over them.

The carbon–chloride pair correlation function calculated from the simulations is displayed as the top curve in Figure 4. The prominent first peak in this function is at 3.7 Å, with a significant shoulder at 4.1 Å. The maximum corresponds to chloride atoms occupying the positions in the first hydration

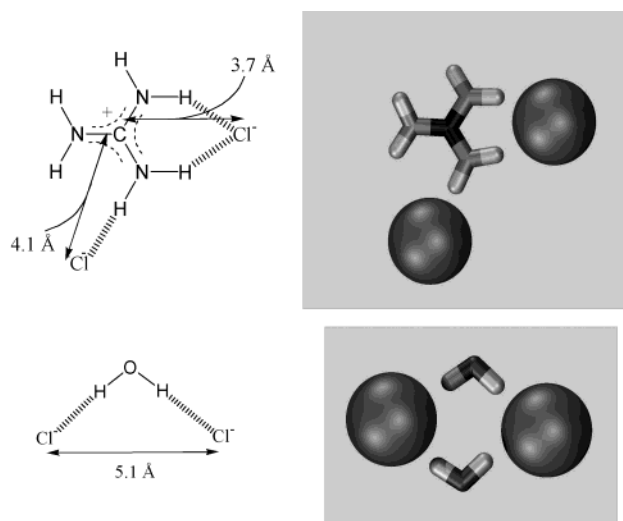


Figure 5. The dominant forms of $\text{Gdm}^+ - \text{Cl}^-$ (upper) and $\text{Cl}^- - \text{Cl}^-$ (lower) ion pairing found in the simulations of GdmCl solution; these lead to the peaks found in the radial distribution functions $g_{CCl}(r)$, $g_{ClCl}(r)$, and $g_{OO}(r)$. At left are shown the schematic arrangements with measurements of inter-ion distances. On the right are shown some representative snapshots from the MD trajectory.

shell between the hydrogen atoms of the guanidinium, hydrogen bonding to both at an angle of 140° (see Figure 5). The shoulder corresponds to chloride ions making a single linear hydrogen bond to a single proton of the guanidinium (also shown in Figure 5). The second peak in the correlation function is at a distance of 6.2 Å and corresponds to the chlorides in the second shell of density visible in the right-hand panel of Figure 2.

The chloride–chloride pair correlation function is shown as the middle curve in Figure 4. The first maximum in this function is at 5.1 Å, which corresponds to two chloride ions mutually coordinated to an intervening water molecule at approximately the tetrahedral angle (see Figure 5). In agreement with the MD simulations of Guàrdia et al.,⁴² no significant direct chloride ion pairing was observed under these conditions.^{29,43} The second peak in the present correlation function falls at 7.4 Å and corresponds to chlorides occupying adjacent positions in the first hydration shell of a guanidinium ion (see Figure 2).

The simulations reveal a significant tendency for the Gdm^+ ions to self-associate in a stacking fashion. The bottom curve of Figure 4 displays the Gdm^+ carbon–carbon pair correlation function, and the middle panel of Figure 2 shows the density of other Gdm^+ ions relative to a central reference ion at three different contour levels. The broad first peak in $g_{CC}(r)$ is at a distance of 4.0 Å, which is larger than the van der Waals contact distance, but which is not sufficiently far apart to allow water molecules to interpose themselves between two ions. It is interesting that this distance is approximately 0.6 Å greater than the minima in the PMFs previously calculated from MC simulations using various water models.²⁷ While there are several differences between the two studies, probably the most significant of these is that the PMF calculations were done on a single guanidinium pair (infinite dilution at finite concentration) and did not include counterions, while here a solution at 3 m concentration with counterions was modeled. It would seem

(42) Guàrdia, E.; Rey, R.; Padró, J. A. *J. Chem. Phys.* **1991**, *95*, 2823–2831.
 (43) Dang, L. X.; Pettitt, B. M.; Rossky, P. J. *J. Chem. Phys.* **1992**, *96*, 4046–4047.

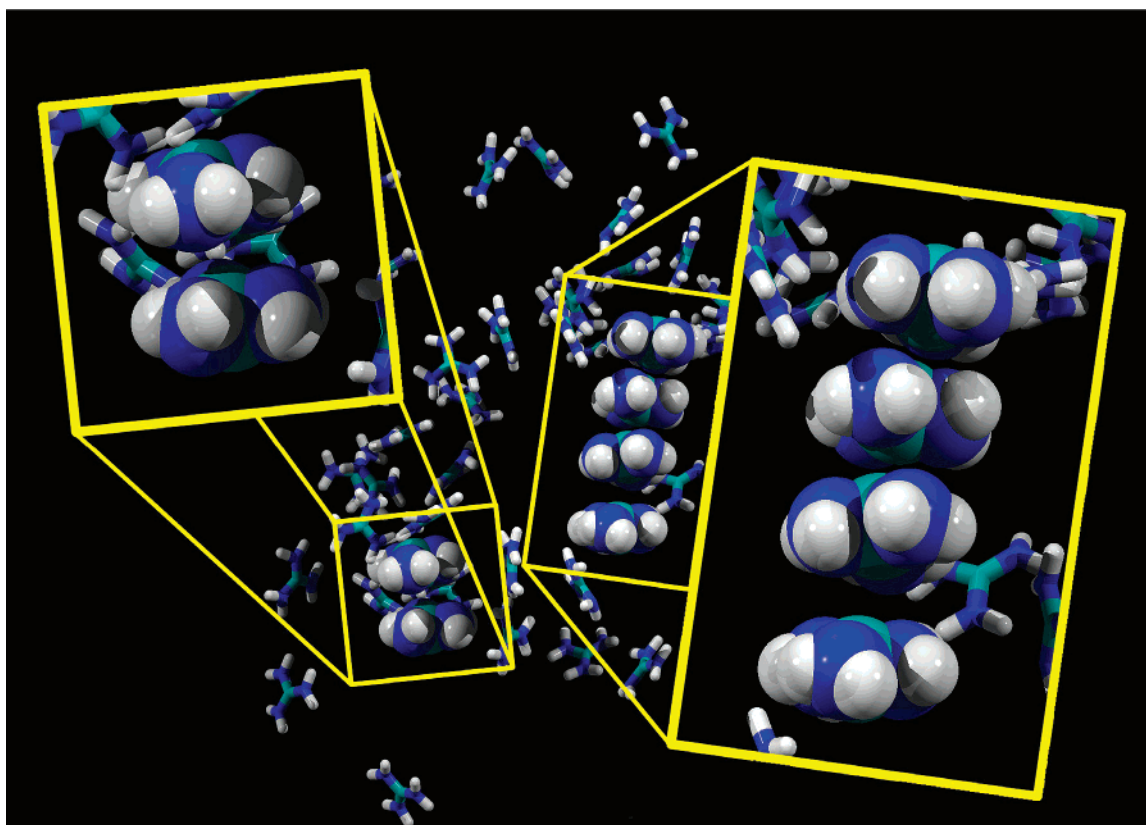


Figure 6. A typical snapshot of the van der Waals surface representation of guanidinium ion positions taken from the MD simulation illustrating a stacked dimer and tetramer.

plausible that the increased separation in the present simulations might be due to the presence of the chloride counterions coordinated to the guanidiniums, which presumably more realistically mimics the experimental regimen. The possibility that counterions may affect the guanidinium pairing is also consistent with previous evidence that denaturants function via direct interaction with proteins rather than by modification of the water structure.^{3,15,16}

The observed stacking also leads to some degree of longer-range directional ordering, as can be seen from Figure 2, although this correlation is much weaker. Figure 6 illustrates typical examples of a stacked dimer and a stacked tetramer taken from a sample snapshot of the simulation. A minimum in the density distribution for carbon atoms displayed in Figure 2 in the direction normal to the plane of the ring was found at 5.1 Å. Using this distance as a cutoff criterion in defining a stacked pair, the populations of clusters of various sizes were calculated and are displayed in histogram fashion in Figure 7. Averaged over the trajectory, about one-quarter (26%) of the guanidinium ions are in dimers, which make up 17% of the *n*-mers (monomers, dimers, etc.). On average, only 3.9% of the guanidinium ions were found in tetramers, which made up only 1.3% of the aggregates. The average lifetime of guanidinium pairs was calculated using the procedure of Rapaport⁴⁴ from the decay of the associational correlation function and was found to be 29 ps.

From inspection, there appears to be a very slight tendency for the stacked guanidinium ions to be slightly off-center, as seen in Figure 6. However, if there is such a tendency, it is

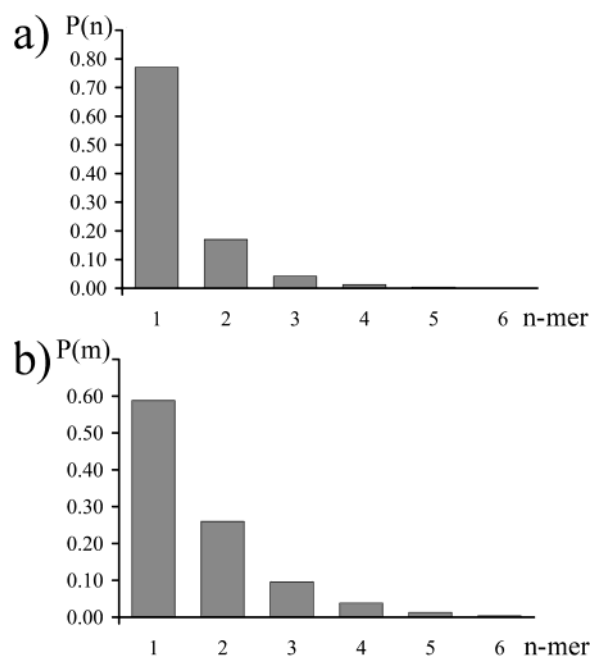


Figure 7. Distribution of populations of guanidinium stacked clusters or *n*-mers of various sizes. Top: percentages of clusters of different sizes. Bottom: probability of guanidinium ions being in an *n*-mer of each size.

sufficiently small that it is not reflected in the broad first peaks of the $g_{CC}(r)$ and $g_{NC}(r)$ radial correlation functions, which occur at approximately the same distances. If such a weak tendency to be stacked off-center is real, it might result from electrostatic attractions between the negative partial charge of the nitrogen atoms and the positive partial charge of the carbon atom.

(44) Rapaport, D. C. *Mol. Phys.* **1983**, *50*, 1151–1162.

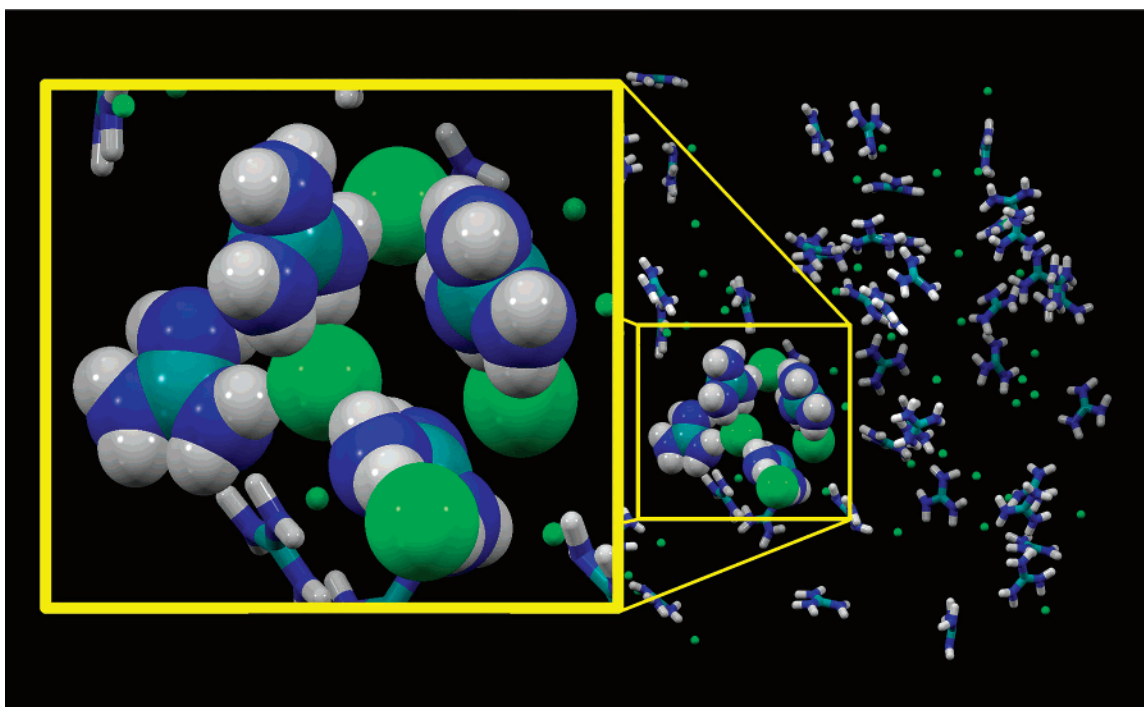


Figure 8. A typical snapshot illustrating a typical hetero-ion cluster.

The most satisfactory explanation for the observed stacking relates to the relative deficiency of hydrating waters directly above and below the plane of the Gdm^+ ion; that is, the ions are drawn to stack by hydrophobic association and are forced together by the external pressure, shrinking the intervening volume, until this tendency is balanced by the electrostatic repulsions of the like-charged ions. Relatively close approaches of the positively charged ions may be promoted by the tendency for Cl^- ions to occupy equatorial positions in the Gdm^+ plane, diminishing inter-ion repulsion of adjacent Gdm^+ ions.⁴⁵ The simulations reveal no significant tendency for the ions to adopt either staggered or eclipsed orientations.

Hetero-ion complexes in which a single chloride ion bridged between two guanidinium ions were found to be common. The guanidinium–guanidinium association in such cases is qualitatively very different from that seen in the direct hydrophobic-like stacking. Not only is the carbon–carbon distance between the two cations much longer, typically greater than 7 Å, but the cations are not in direct contact or oriented in a parallel fashion, as can be seen from Figure 8. This hetero-ion pairing is considerably stronger than the hydrophobic-like guanidinium homo-ion pairing. Because many of the guanidinium cations bind to more than one chloride counterion, irregularly structured short chains of alternating chloride and guanidinium ions frequently arise. The rich ion pairing found in this solution provides an interesting microscopic rationale for the nonideality of solution properties.

The collective structure of the present solution was thus quite complex and dynamic. Figure 9 displays a single snapshot of the simulation depicting all atoms in the primary box. The conventional atomic color-coding in this figure is modified for clarity in that those guanidinium ions participating in homo-ion clusters are colored entirely red; as can be seen, this snapshot

contains several such dimers and at least two trimers. Some of the oligomeric hetero-ion clusters have also been highlighted in purple. A movie in which another frame of the box taken from the simulation is rotated for clarity, both with and without the water molecules displayed, is included in the Supporting Information. In this movie, at least two examples of alternating hetero-ion chains are illustrated with the ions colored purple.

The simulation results observed here are robust with respect to the various approximations involved in the model. For example, it was found that the general features of the structuring reported here were insensitive to the water force field (the same result was obtained with SPC/E water), and relatively insensitive to the Ewald parameters used. As already noted, they are also insensitive to the intramolecular potential energy function, with a completely rigid solute giving the same intermolecular correlations as the most flexible parameter set studied.

The interesting tendency for the like-charged Gdm^+ ions to self-associate, as well as their reasonably strong hydrogen bonding to water and chloride counterions, suggests why this ion is so effective as a protein denaturant. The equator of the molecule interacts preferentially with water molecules, while the faces preferentially interact with hydrophobic surfaces. This hydrophobic property of guanidinium is entirely consistent with the observation in protein crystal structures of planar stacking interactions of aromatic amino acid side chains with the guanidine group of arginine.⁴⁶ The resulting augmentation of the solubility of hydrophobic groups leads to the folding/denaturation equilibrium being shifted in favor of the denatured state. The effect is weak and thus requires high concentrations of guanidinium to be an effective denaturant, such as the 3 *m* solutions studied here. This hydrophobic association is likely to accompany favorable hydrogen-bonding interactions made by the equatorial N–H groups of Gdm^+ with the weakly hydrated backbone amide groups that are also exposed on

(45) Angelini, T. E.; Liang, H.; Wriggers, W.; Wong, G. C. L. *Proc. Natl. Acad. Sci. U.S.A.* **2003**, *100*, 8634–8637.

(46) Flocco, M. M.; Mowbray, S. L. *J. Mol. Biol.* **1994**, *235*, 709–717.

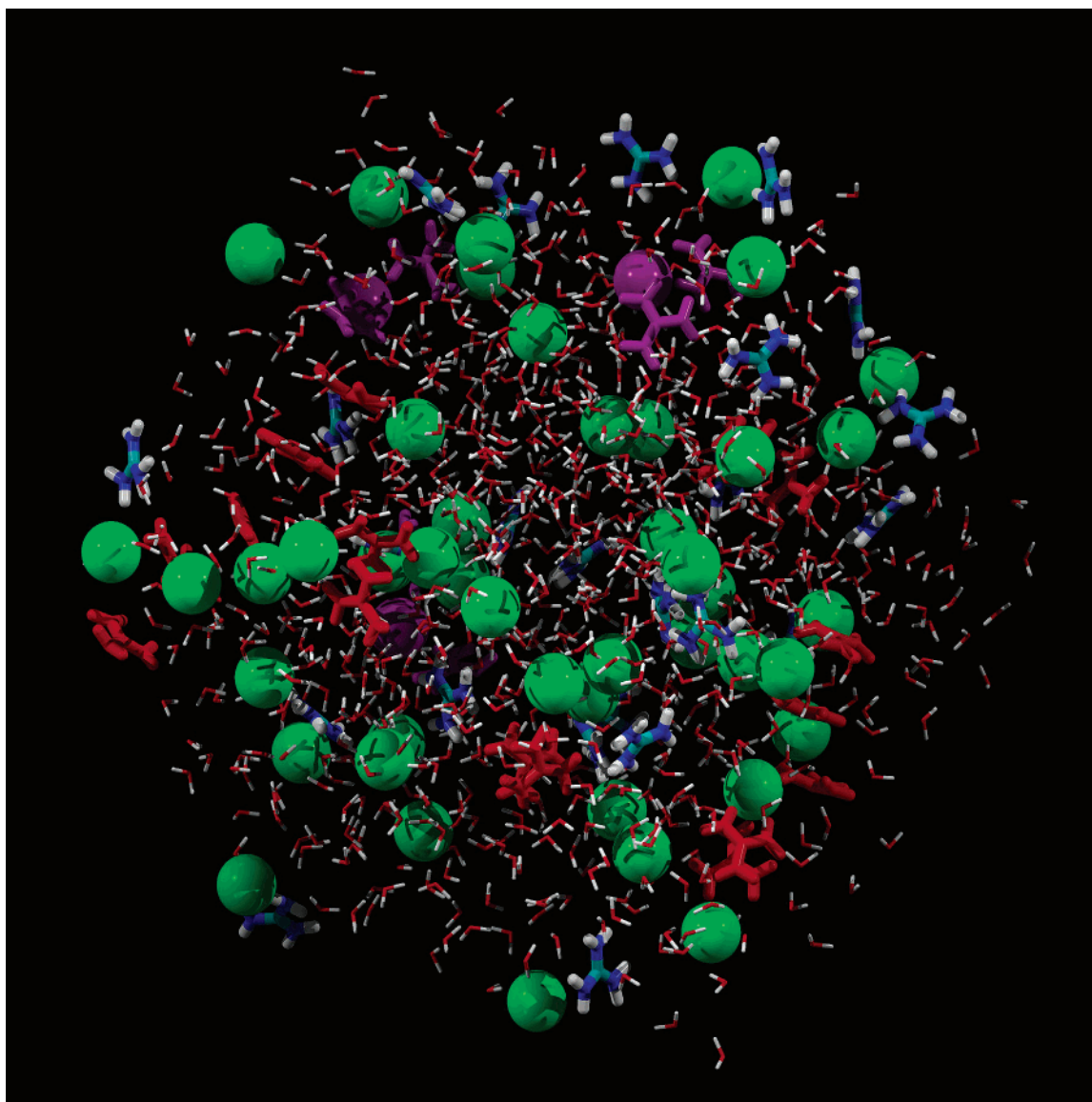


Figure 9. A typical snapshot of all atoms in the primary simulation box taken from the simulation. All guanidinium ions participating in stacked homo-ion clusters are colored red, and several selected hetero-ion clusters are highlighted in purple.

protein unfolding.^{47,48} From this molecular level explanation of the functioning of the denaturant Gdm^+ , it might be predicted that the observed stacking would be affected by the counterion: for example, GdmCl (a powerful denaturant) would have a greater level of stacking than Gdm_2SO_4 (a mild protein stabilizer). In addition, the ion stacking predicted by the MD simulations could be tested because certain structural features characteristic of this stacking could be examined through further specific neutron scattering experiments.

Conclusions

The present combination of MD simulations and neutron diffraction data has allowed for an analysis of the structuring in guanidinium chloride solutions and provided an experimental validation of the general features of the computational modeling. Comparison of the calculated and experimental structure through radial distribution functions suggested that the intramolecular

parameters used in the initial simulation produced a guanidinium molecule that was too rigid. In principle, such information could be used to improve the force field through iterative revision of the bond stretching and bending constants until better agreement with the diffraction experiment was achieved. Soper has described the use of MM calculations in the interpretation of diffraction results and their iterative use in the revision of parameters.^{49,50} In the present case, the suggestion based on the experiments that the guanidinium ions in the simulations might be too rigid prompted us to reexamine these constants using high-level ab initio calculations, and the initial set was actually found to be too flexible. However, the diffraction data are resolution-limited, and not very sensitive to these parameters, as was subsequently determined by the MD simulations. For this reason, the ab initio data alone were used in revising the force constants, because it is more reliable and provides better agreement with the much more sensitive vibrational data.

(47) Zou, Q.; Habermann-Rottinghaus, S. M.; Murphy, K. P. *Proteins* **1998**, *31*, 107–115.

(48) Makhatadze, G. I.; Privalov, P. L. *J. Mol. Biol.* **1992**, *226*, 491–505.

(49) Dixit, S.; Crain, J.; Poon, W. C. K.; Finney, J. L.; Soper, A. K. *Nature* **2002**, *416*, 829–832.

(50) Soper, A. K. *Mol. Phys.* **2001**, *99*, 1503–1516.

The structure of guanidinium chloride solutions was found to be complex indeed, with significant ion pairing for the like-charged guanidinium ions and with regular, and in retrospect, predictable organization of the solvent and chloride counterions around the guanidinium ions. The somewhat surprising tendency of the guanidinium ions to pair, in agreement with previous Monte Carlo calculations of the PMFs for two guanidinium ions in an infinitely dilute solution, suggests a plausible mechanism for the protein denaturing ability of guanidinium chloride. In this picture, the guanidinium ions can associate with hydrophobic groups such as the side chains of tryptophan, tyrosine, and phenylalanine through hydrophobic association, while simultaneously making hydrogen bonds with water and polar functional groups in the protein, thus reducing the tendency for self-association and reducing the penalty for unfolding in the presence of water. The possible role of the bound chloride ions in allowing the guanidinium ions to associate would be

consistent with the observation that the effectiveness of guanidinium as a denaturant in water depends on its counterion. Experiments are planned to search for the signatures of guanidinium hydrophobic binding to proteins to test this proposed denaturation mechanism.

Acknowledgment. We thank Dr. A. C. Barnes and Prof. A. K. Soper for their helpful discussions. This project was supported by grants from the National Institutes of Health (GM63018 to J.W.B. and GM51501 to A.D.M.) and from the EPSRC.

Supporting Information Available: New force field parameters and a movie depicting the structure of the simulated solution (AVI). This material is available free of charge via the Internet at <http://pubs.acs.org>.

JA040034X